doi:10.1016/j.jmb.2004.10.049 J. Mol. Biol. (2005) 345, 351–361

JMB

Available online at www.sciencedirect.com

SCIENCE DIRECT®

ELSEVIER

# Assembly of *Acanthamoeba* Myosin-II Minifilaments. Definition of C-terminal Residues Required to Form Coiled-coils, Dimers, and Octamers

**Kirsi Turbedsky* and Thomas D. Pollard**

*Structural Biology Laboratory Salk Institute for Biological Studies, 10010 North Torrey Pines Road, La Jolla, CA 92037 USA*

**Corresponding author*

*Acanthamoeba* myosin-II forms bipolar octamers by three successive steps of dimerization of the C-terminal, coiled-coil tail. In this study, we generated N-terminal and C-terminal truncation constructs and point mutants of the *Acanthamoeba* myosin-II tail to delineate the structural requirements for assembly of bipolar mini-filaments. By the use of light-scattering, CD spectroscopy, analytical ultracentrifugation, and tryptophan fluorescence experiments, we determined that: (1) the C-terminal 14 heptad repeats plus most of the tailpiece (residues 1381–1509) are required to form antiparallel dimers of coiled-coils; (2) amino acid residues within heptads 23–32 (residues 1254–1325) are required to form tetramers; (3) the C-terminal 32 heptad repeats suffice to assemble octameric minifilaments; (4) A1378 is outside of the interaction interface; (5) the mutation L1475W inhibits dimerization; and (6) F1443 is involved in the dimerization interface but is exposed to the solvent. We propose that the tailpiece (residues 1483–1509) interacts with two heptads (13 and 14, residues 1381–1393), which are important for dimerization and coiled-coil formation. These results support a model in which hydrophobic as well as electrostatic interactions control the register between myosin-II coiled-coils and guide sequential steps of dimerization that generate stable, octameric mini-filaments.



*Keywords:* myosin; coiled-coil; assembly; analytical ultracentrifugation; light-scattering

## Introduction

*Acanthamoeba* myosin-II provides an attractive system to study the assembly of bipolar filaments, because these minifilaments consist of only eight monomers and the assembly pathway is well characterized.[1–3] Two myosin monomers bind very rapidly ($k^+ > 10^8\,M^{-1}\,s^{-1}$) and with high affinity ($K_d < 10^{-11}\,M$) to form antiparallel dimers with an overlap of ~15 nm (Figure 1). Two antiparallel dimers associate with another ~15 nm stagger to form an antiparallel tetramer. Finally, two tetramers bind with a ~30 nm stagger to form octamers. In millimolar concentrations of divalent cations or at acid pH, minifilaments associate laterally to form thick filaments. Both minifilaments and thick filaments have been observed in fixed[4] and in live cells.[5]

The *Acanthamoeba* myosin-II tail, like other type-II myosins, contains extensive heptad repeats of hydrophobic residues characteristic of coiled-coils (Figure 2),[6] as well as 28 residue charge repeats implicated in defining the ~14.3 nm stagger of molecules within myosin filaments.[6–8] The middle of the *Acanthamoeba* myosin-II tail has a helix-breaking proline residue (Pro1244) surrounded by ~20 residues with low propensity to form α-helix. This hinge region results in a statistically significant bend in electron micrographs of *Acanthamoeba* myosin-II monomers.[6] A second proline residue (Pro1483) initiates the non-helical tailpiece, which consists of the last 27 residues and contains multiple serine and glycine residues instead of the coiled-coil heptad repeat.[9]

Previous work identified the critical role of the C-terminal end of the myosin-II tail in assembly. Studies using 25 different monoclonal antibodies with mapped epitopes and nine C-terminal truncations identified regions of the coiled-coil tail

Present address: T. D. Pollard, Department of Molecular, Cellular and Developmental Biology, Yale University, New Haven, CT 06520, USA

Abbreviations used: RMS, root-mean-square.

E-mail address of the corresponding author: turbedsky@access4less.net

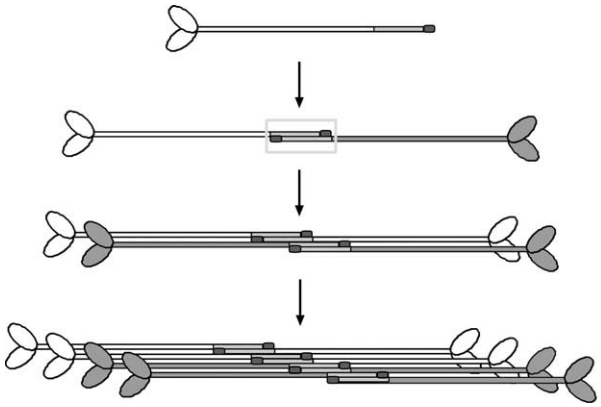

**Figure 1.** Two-dimensional drawing of the assembly pathway of *Acanthamoeba* myosin-II consisting of three steps of successive dimerization of α-helical coiled-coils to form octameric minifilaments.[2] The boxed region in the first dimerization step shows the predicted dimer formed by construct 15T. In the first assembly step, anti-parallel dimerization of two coiled-coils involves an overlap of ~15 nm. The non-helical tailpieces (black) are essential for the first step of assembly and comprise residues 1483–1509. The maximum overlap between antiparallel molecules in tetramers is ~30 nm.

involved in each step of *Acanthamoeba* myosin-II assembly.[10,11] For example, antibodies that bind tightly in the last 37 nm of the tail or deletion of more than 100 residues at the C terminus precluded assembly. In electron micrographs of *Acanthamoeba* myosin-II at high concentrations of salt, the tailpiece of one myosin occasionally associates with another myosin tail ~15.0 nm from the C terminus.[12] Constructs missing as few as 15 residues from the tailpiece do not form antiparallel dimers but are capable of making parallel dimers with a stagger similar to that observed for tetramers. In addition, monoclonal antibodies that bind near residue 1380, ~15.0 nm from the C terminus, inhibit the anti-parallel dimerization of myosin-II.[10] Therefore, the tailpiece (residues 1483–1509) is clearly essential for step 1 of assembly. Further experiments using monoclonal antibodies show that residues between 1380 and 1481 are involved in formation of the ~15 nm stagger in step 2, and that residues between 1280 and 1380 are important in step 3.

Here, we performed biophysical measurements of recombinant N-terminal and C-terminal constructs to define the regions within the myosin-II tail that are required for assembly. We tested N-terminal truncation constructs and point mutations to determine the minimal sequence required to form specific assembly intermediates. By the use of light-scattering, CD spectroscopy, analytical ultracentrifugation, and tryptophan fluorescence, we determined that the C-terminal 32 heptad repeats suffice to assemble octamers, while the C-terminal 14 heptad repeats plus most of the tailpiece are required to form dimers. In addition, we show that residues 1381–1393 are involved in dimerization and coiled-coil formation.

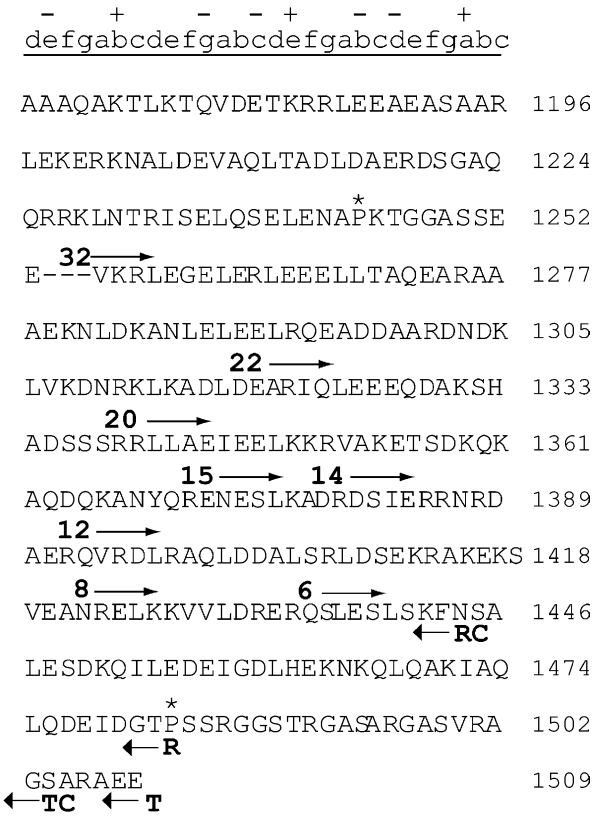


**Figure 2.** Amino acid sequence of the C terminus of the *Acanthamoeba* myosin-II tail showing the primer start sites for construct design. Bold numbers with arrows above the sequence indicate the N-terminal primer start sites, while bold letters with arrows below the sequence indicate the C-terminal primer start sites. The top row lists the predominant charge repeat pattern (±) in the 28 residue repeats and the heptad repeat (a–g). Asterisks (*) mark proline 1244 (hinge region) and proline 1483 (tailpiece start site).

## Results

### Design and purification of constructs

We designed a series of N-terminal and C-terminal truncation constructs of the *Acanthamoeba* myosin-II tail on the basis of assembly and stability criteria to examine the structural requirements for assembly of bipolar filaments. Computational algorithms[13,14] predicted that the coiled-coil begins after Pro847 and ends at Pro1483, encompassing a total of 90 heptad repeats. Our longest construct with 32 heptads (32T) begins at residue 1254 and was predicted to form dimers and tetramers. This 34 nm coiled-coil is only 40% of the tail but is longer than the maximum ~30 nm overlap between antiparallel molecules in tetramers (Figures 1 and 3). Furthermore, monoclonal antibodies binding within this region, but not those binding further toward the N terminus, inhibit assembly.[10] This construct avoids the hinge region of the tail surrounding Pro1244, which has much

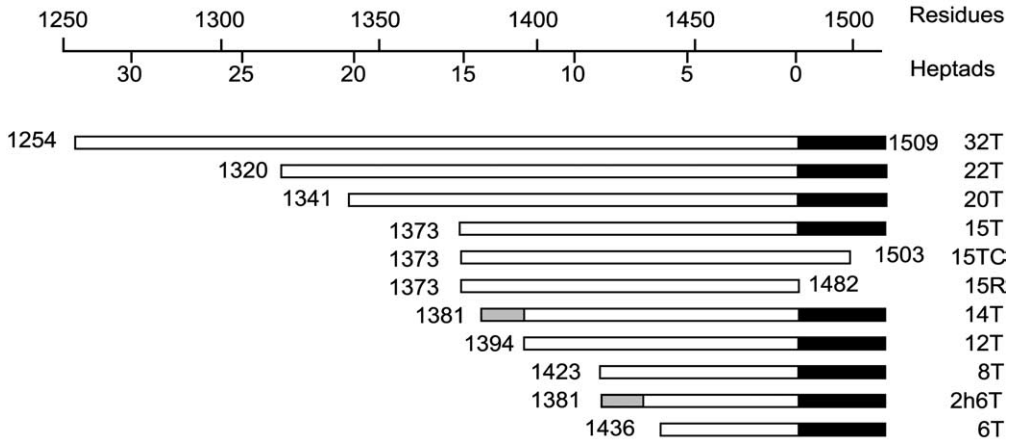


**Figure 3.** A representation of myosin tail constructs showing their N and C termini. The tailpiece is black and heptads 13/14 are shaded gray in construct 14T and 2h6T. The lengths of the coiled-coils (1254–1482) are calculated assuming a rise of 1.5 Å/residue.

lower coiled-coil probability and is expected to be a less structured coiled-coil.[6] The shortest construct, 6T, begins at residue 1436 and was expected to be too short to form dimers or higher-order assemblies. However, a comparison with GCN4 and synthetic consensus sequence peptides[15,16] suggested that 6T should be long enough to form a stable coiled-coil owing to a leucine residue in each d position and an asparagine residue in one a position. Constructs intermediate in length between 6T and 32T were designed to test particular features of the assembly model (Figure 2). Constructs 12T, 14T and 15T were designed to approximate the 15 nm overlap observed in the first step of assembly and to determine the minimum N-terminal sequence required for tailpiece binding to the partner coiled-coil in the dimer. If the coiled-coil overlap were precisely 15 nm, then constructs that began before residue 1360 were predicted to form anti-parallel dimers, while constructs that began after residue 1400 were predicted to be monomeric.

The sequence of the tailpiece (residues 1483–1509) was not predicted to form a coiled-coil or have any clearly defined secondary structure. Previous work demonstrated that constructs lacking the last 67 residues, including the tailpiece, form parallel dimers, similar to the second step of assembly.[11,17] Since the tailpiece is required for the first anti-parallel step in assembly, we tested the assembly of the 15-heptad construct lacking all of the tailpiece (15R) or the last seven residues that can be cleaved by chymotrypsin (15TC).[9]

*Escherichia coli* expressed all of the myosin-II tail constructs in abundance, yielding tens to hundreds of milligrams of pure protein, free of nucleic acid contamination after purification by boiling and ion-exchange chromatography (Figure 4). Further purification of construct 15T on a Mono S cation-exchange column revealed multiple peaks that eluted at 72 mM KCl, 80 mM KCl, and 88 mM KCl (Figure 5(a)), each of which ran true upon re-chromatography on the same Mono S column (Figure 5(b)). The protein in these fractions had the same mobility on SDS-PAGE, but isoelectric focusing separated the protein into three bands with isoelectric points of 7.0, 6.5, and 6.3 (Figure 5(c)). When separated from each other, these three charge species assembled identically.

## Assay for assembly

We used sedimentation equilibrium analytical ultracentrifugation to determine the oligomeric species formed by our myosin-II tail constructs over a broad range of concentrations (0 to 500 mM) of KCl. We refer to myosin tail molecules consisting of two helical chains forming a coiled-coil as monomers and single polypeptide chains ("half" of a monomer) as single chains. A single species fit to the data provided the *z*-average molecular mass ($M_z$). For a simple ideal system, $M_z = M_w$ (weight average molecular mass), but in an associating system, $M_z$ is weighted toward the largest species. The ratio of $M_z/M_{mono}$ (where $M_{mono}$ is the molecular mass of a monomeric coiled-coil) varied between 0.5 and 8, depending on the concentration of salt and the length of construct (Table 1). $M_z/M_{mono}$ is less than 1 for constructs shorter than 14T, indicating that the shortest constructs did not form coiled-coils. For samples that assembled ($M_z/M_{mono} > 1$), the data were fit using WinNonlin software to determine the equilibrium constant between the oligomeric species (Table 1). Due to the lack of an absorbance signal and the low sensitivity of interference optics, measurements were collected at myosin concentrations much greater than the $K_d$. Consequently, the $K_d$ values are only approximate.

## N-terminal structural requirements for assembly

Analytical ultracentrifugation and light-scattering showed that construct 32T forms octameric mini-filaments with the same intermediates as full-length

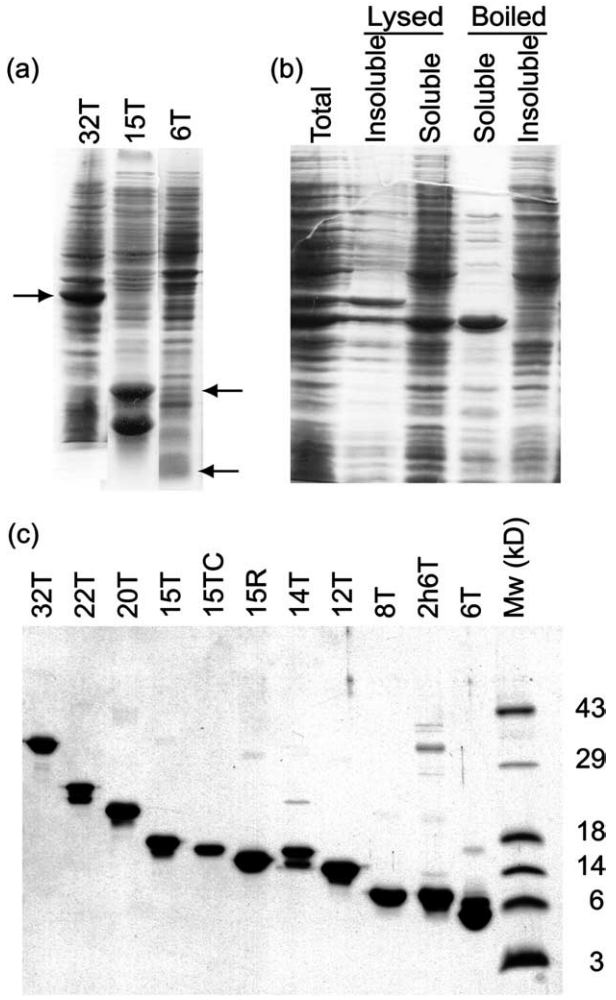


**Figure 4.** Bacterial expression and purification of truncation constructs. SDS-PAGE of purified samples stained with Coomassie brilliant blue. (a) Whole cell lysates of constructs expressed in *E. coli* using the pMW172 vector. Arrows indicate the expected sizes of the expressed proteins. (b) Purification of construct 32T. Most 32T was soluble after lysis in 10 mM Tris, 10 mM EDTA, 10% (w/v) sucrose, 0.01% (v/v) Triton X-100, 1 mg/ml of lysozyme, 1 mM PMSF. Upon boiling the soluble extract, most bacterial proteins precipitated, leaving the soluble fraction enriched in 32T, which was purified further by cation-exchange chromatography. (c) Purity of each of the constructs used in this study.

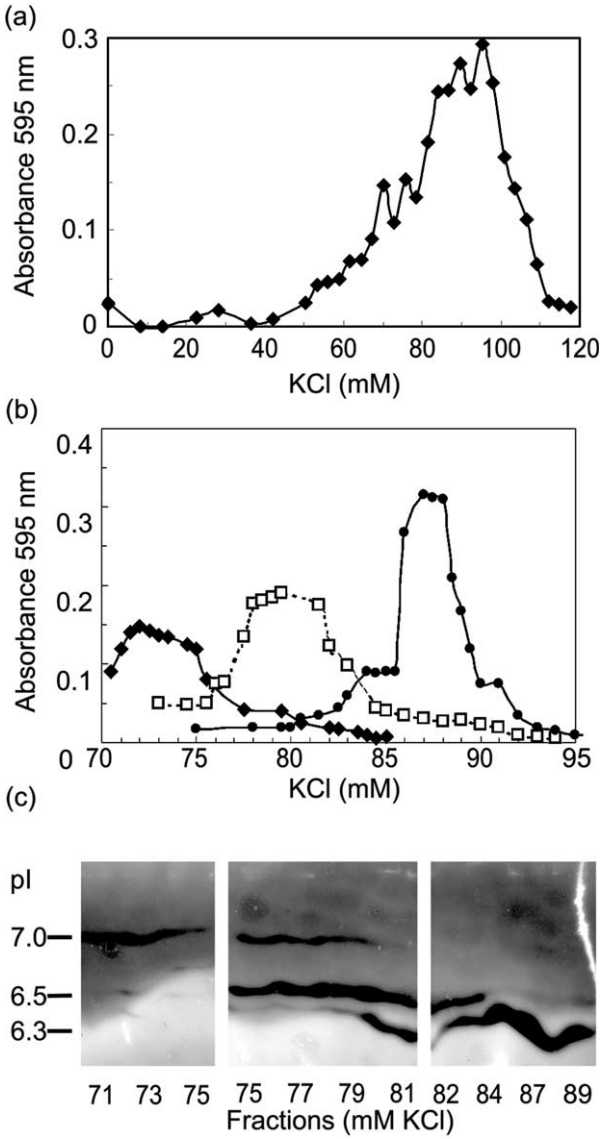


**Figure 5.** Purification of 15T by cation-exchange chromatography and analysis by isoelectric focusing. (a) Elution of 15T from a 10 cm Mono S column with a gradient of 0–120 mM KCl in 20 mM imidazole (pH 7), 1 mM EDTA. The sample was collected in three pools (a, 60–75 mM; b, 75–85 mM; and c, 85–100 mM KCl). (b) Re-chromatography of the three 15T pools (a, filled diamonds; b, open squares; c, filled circles) on the Mono S column. The pools remained distinct, centered around 72 mM KCl, 80 mM KCl and 88 mM KCl, respectively. (c) Isoelectric focusing shows that the fractions from the chromatography elution profile shown in (a) contain charged species with isoelectric points of 6.3, 6.5, and 7.0.

myosin-II. In 500 mM KCl, the $M_z/M_{mono}$ of 32T was 2.4, which fit well to an equilibrium between dimer and tetramer, two very stable intermediates in the assembly pathway.[2] The existence of weakly associated dimers and tetramers in high salt was not observed for native myosin-II, since only lower concentrations of protein were examined. At lower concentrations of salt, $M_z/M_{mono}$ rose to 7.4, indicating the presence of larger species in solution. In 0 or 100 mM KCl, the sedimentation curves fit best to an equilibrium between tetramers and octamers with a sub-micromolar $K_d$. Octamers were favored somewhat more in 100 mM KCl compared with no salt, similar to full-length myosin-II. No species larger than octamers was detected. In spite of its small size (native molecular mass of 58 kDa), 32T scattered light at 365 nm in a salt-dependent manner with a maximum signal around 50 mM KCl (Figure 6(a)), similar to full-length myosin-II (molecular mass 400 kDa). Like full-length myosin,[1] 32T formed large aggregates in

**Table 1.** Predominant oligomeric state as a function of salt concentration determined by analytical ultracentrifugation

| | Salt concentration (mM) | | | | | | | | | |
|---|---|---|---|---|---|---|---|---|---|---|
| | 0 | | | 100 | | | 500 | | | |
| | $M_z/M_{mono}$ | Species | $K_d$ (μM) | $M_z/M_{mono}$ | Species | $K_d$ (μM) | $M_z/M_{mono}$ | Species | $K_d$ (μM) |
| 32T | 7.03 | T-O | 3 | 7.36 | T-O | 0.08 | 2.42 | D-T | 25 |
| 22T | 2.29 | M-D | 1 | 2.02 | M-D | 0.2 | 1.69 | M-D | 12 |
| 20T | 2.01 | D-T | 35 | – | – | – | – | – | – |
| 15T | 1.76 | M-D | 9 | 1.91 | M-D | 5 | 1.62 | M-D | 5 |
| 15TC | 1.69 | M-D | 11 | 1.84 | M-D | 14 | 1.33 | M-D | 120 |
| 15R | 2.09 | M-D | 7 | 1.96 | M-D | 5 | 1.76 | M-D | 33 |
| 14T | 1.66 | M-D | 56 | 1.11 | M-D | 62 | 0.88 | M-D | 108 |
| 12T | 0.68 | SC-M | 530 | 0.45 | SC-M | 430 | 0.60 | SC-M | 700 |
| 8T | 0.76 | SC-M | 260 | 0.72 | SC-M | 420 | 0.69 | SC-M | 600 |
| 2h6T | 0.76 | SC-M | 440 | 0.78 | SC-M | 270 | 0.70 | SC-M | 620 |
| 6T | 0.51 | SC | – | 0.70 | SC-M | 5000 | 0.68 | SC-M | 5000 |

SC, single chain; M, monomer; D, dimer; T, tetramer; O, octamer.

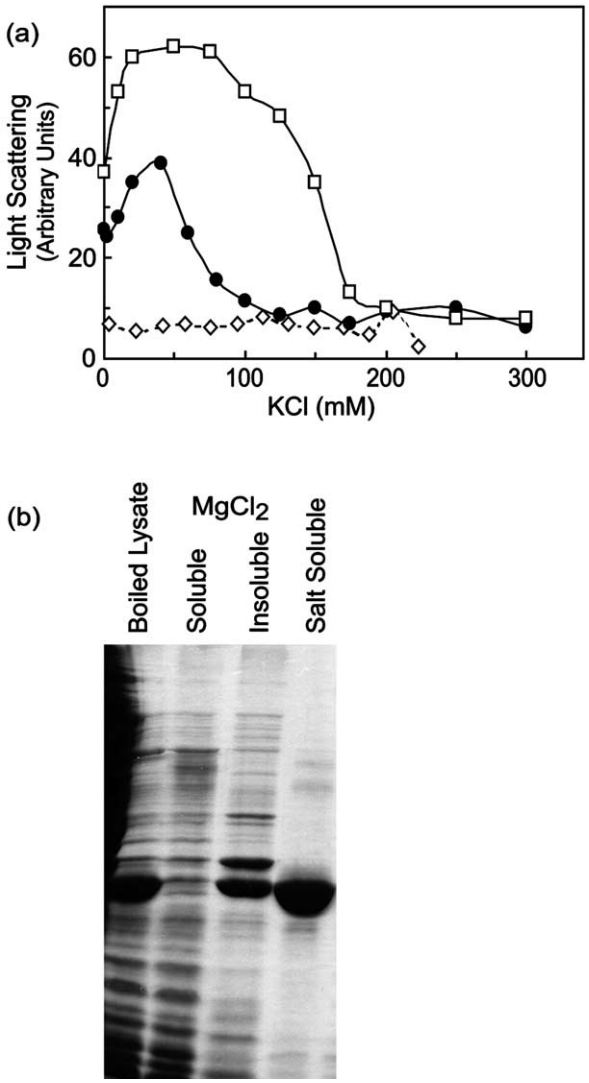


**Figure 6.** Assembly of 32T observed by light-scattering and aggregation in $MgCl_2$. (a) Light-scattering of 32T and 15T as a function of salt. Construct 32T (circles) at 0.15 mg/ml had a measurable 90° light-scattering signal at 365 nm below 75 mM KCl, while construct 15T (diamonds) at 0.2 mg/ml did not. For comparison, the scattering profile of *Acanthamoeba* myosin-II (squares) as published is included.[12] The relative amplitudes of the signals of 32T and myosin-II were not determined. (b) Purification of 32T by precipitation in $MgCl_2$. Boiled Lysate: soluble fraction of cells overexpressing 32T after boiling for ten minutes, incubation on ice for one hour, and centrifugation at 75,000*g* for one hour. $MgCl_2$ Soluble and $MgCl_2$ Insoluble: boiled lysate was dialyzed into 20 mM Tris (pH 7.5), 5 mM $MgCl_2$ overnight and centrifuged at 6000*g* for 15 minutes. Salt Soluble: soluble fraction after resuspending the $MgCl_2$-insoluble pellet in 10 mM Hepes (pH 8), 40 mM sodium pyrophosphate, 10 mM EDTA and clarification at 6000*g* for 15 minutes.

10 mM $MgCl_2$. We exploited this property for purification (Figure 6(b)).

Constructs 22T and 20T did not form octamers or tetramers. Instead, they each formed predominantly dimers with binding affinities that increased

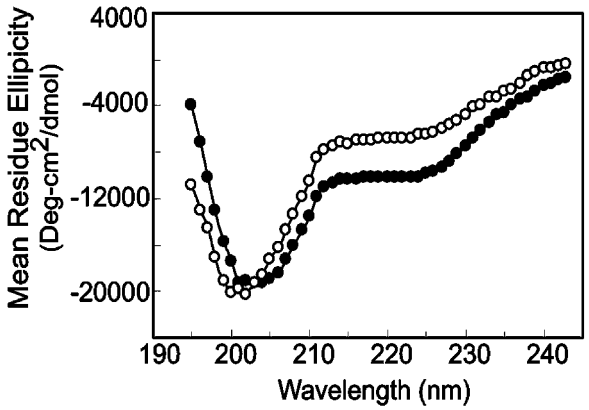


**Figure 7.** The CD spectra of construct 6T collected in 5 mM (open circles) and 200 mM (filled circles) pyrophosphate buffer. The amplitude of the trough at ~202 nm is much smaller than expected for a coiled-coil (−34,000 deg cm$^2$/dmol).

at lower concentrations of salt. Neither construct precipitated in the presence of $MgCl_2$, confirming the absence of octamers.

Construct 15T formed dimers with a dissociation equilibrium constant of ~5 μM. Construct 14T also formed predominantly dimers but with a slightly weaker affinity. Neither of these constructs had a salt-dependent change in light-scattering nor formed large aggregates in 10 mM $MgCl_2$.

Construct 12T did not form dimers. In fact, under all conditions it formed weak coiled-coils with a significant fraction of protein unfolded. Therefore, the two heptads between 12T and 14T (residues 1381–1393) are important for both coiled-coil formation and the dimerization of coiled-coils.

The smallest constructs, 6T and 8T, did not form coiled-coils. Instead, each was mainly a single chain, even at concentrations of protein as high as 2 mM. CD spectra of 6T showed a low fraction of α-helix but not the hallmark spectral features of a coiled-coil (Figure 7). Deconvolution methods predict the protein contains less than 14% α-helix. For comparison, a fully helical structure would have a molar ellipticity near −34,000 deg cm$^2$/dmol.[18]

Since construct 14T formed coiled-coils more readily than construct 12T, we tested the ability of heptads 13 and 14 (residues 1381–1393) to serve as a "trigger sequence"[19] when added to the N terminus of construct 6T (construct 2h6T). A comparison of the assembly of 2h6T with the construct of identical length (8T) showed that neither heptads 13/14 nor heptads 7/8 enabled 6T to form a coiled-coil (Table 1).

### C-terminal structural requirements required for assembly

Construct 15TC, lacking the last seven residues in the tailpiece, formed dimers like 15T with a full tailpiece, although the affinity was slightly weaker (10–120 μM). Construct 15R, lacking the entire tailpiece, also formed dimers with affinities of 5–30 μM.

### Lateral interactions in dimers

We made three tryptophan substitutions in the coiled-coil of 15T to probe lateral interactions in the anti-parallel dimer (Table 2). Our goal was to introduce a tryptophan residue into a position that would have different fluorescence in the monomeric state *versus* an oligomer. We tested the effect of these substitutions on assembly and the effect of assembly on the fluorescence of these single tryptophan residues (Figure 8). Substitution of tryptophan for Ala1378 (f position) did not affect dimer formation, and the fluorescence of monomers and dimers was identical. Substitution of tryptophan for Leu1475 (d position) strongly inhibited dimer formation. Substitution of tryptophan for Phe1443 (g position) reduced the affinity of dimers tenfold. The tryptophan fluorescence emission peak of F1443W differed by 4 nm in high and low concentrations of salt (Figure 8). This indicates that the environment of F1443W changes upon assembly.

## Discussion

In this study, we generated N-terminal and C-terminal truncation constructs and point mutants of the *Acanthamoeba* myosin-II tail to delineate the structural requirements for formation of the coiled-coil and the assembly of the coiled-coil into dimers, tetramers and octamers. CD spectroscopy revealed the α-helical content of the oligomers, and analytical ultracentrifugation studies documented the size of the products. Lateral interactions between dimers were examined by fluorescence spectroscopy of tryptophan point mutants. The ability of $MgCl_2$ to

**Table 2.** Tryptophan point mutations of construct 15T

| | | Assembly parameters by analytical ultracentrifugation | | Fluorescence peak emission wavelength (nm) | | |
|---|---|---|---|---|---|---|
| Mutation | Heptad position | $M_z/M_{mono}$ | $K_d$ (μM) | 20 mM KCl | 100 mM KCl | Change |
| A1378W | f | 2.02 | 1 | 347 | 347 | 0 |
| F1443W | g | 1.72 | 50 | 342 | 346 | +4 |
| L1475W | d | 1.05 | 280 | 349 | 349 | 0 |
| X1510W | Tailpiece | 1.66 | 10 | 358 | 358 | 0 |

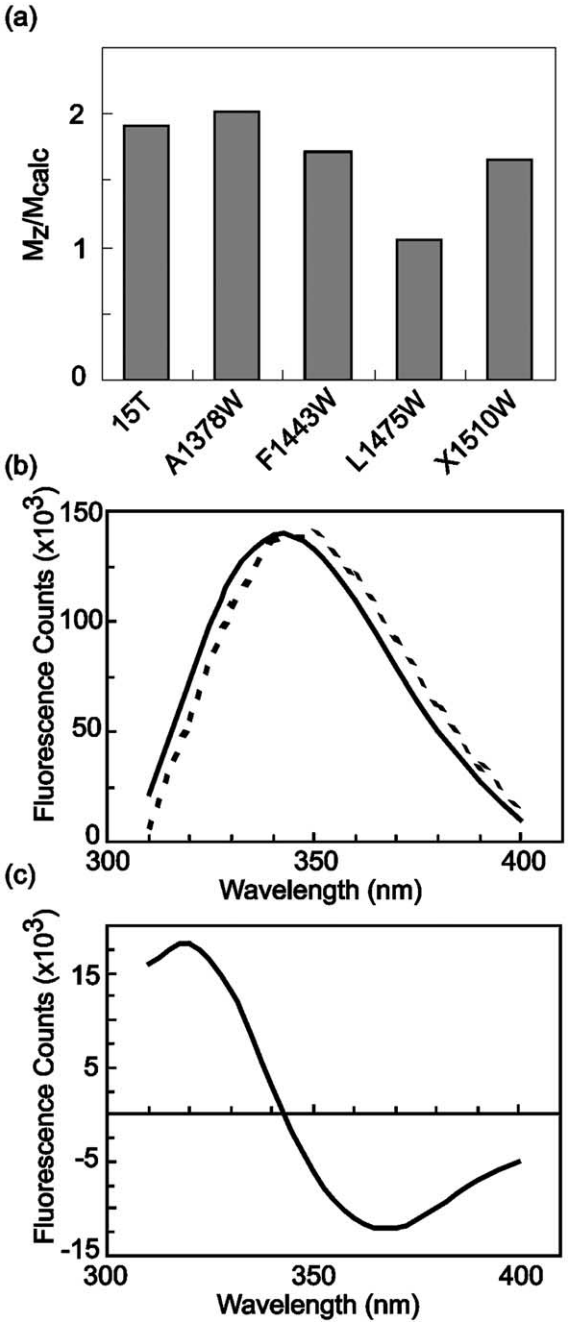


**Figure 8.** Assembly and fluorescence of 15T tryptophan point mutants. (a) $M_z/M_{mono}$ ratios for tryptophan point mutants of 15T as determined by sedimentation equilibrium in 100 mM KCl. All mutants form monomers with a lower tendency to dimerize than 15T. (b) Tryptophan emission spectra of 15T-F1443W (10 μM) in 0 mM KCl (continuous line) and 0.6 M KCl (broken line) with excitation at 290 nm. (c) Difference between the fluorescence in 0 M KCl and 0.6 M KCl. The greatest changes occur at 320 and 365 nm. The ratio of $I_{320nm}/I_{365nm}$ was useful for monitoring the shift.

precipitate the products provided an independent test for native octamers, since $MgCl_2$ aggregates octamers of native myosin-II, but not monomers, dimers or tetramers.[12]

## Requirements to form a coiled-coil

The sequence of 6T suggested that it would form a coiled-coil based on computational prediction and a conventional heptad repeat similar to the GCN4 leucine zipper sequence. However, analytical ultracentrifugation showed that 6T is a single chain rather than a coiled-coil, even at very high concentrations of protein. CD spectroscopy confirmed that construct 6T has only ~14% α-helix content and is most likely unfolded. Even 12T, which contains twice as many heptads, is found mainly as unfolded single chains.

A construct with 14 heptads (14T) was the shortest that produced a stable coiled-coil. Therefore, residues in heptads 13 and 14 appear to contribute significantly to the stability of the coiled-coil. Residues 1381–1393 may simply add the required length of interfacial hydrophobic residues between the helices necessary to hold the chains together or provide the necessary number of heptads for cooperative coiling. However, this sequence has no special hydrophobic character and is expected to be less stable than the GCN4 coiled-coil, in spite of the fact that it stabilizes the coiled-coil.

A second possibility for the difference between 12T and 14T is that residues 1381–1393 serve as a trigger sequence[19] to initiate the formation of the coiled-coil. Trigger sequences are defined as short (two) heptad repeats that are capable of inducing a coiled-coil structure in heptad sequences that do not form coiled-coils on their own. Neither myosin-II residues 1381–1393, nor any other part of the tail, match the loose consensus sequence based on trigger sequences from cortexillin and GCN4. Nevertheless, we tested the ability of heptads 13 and 14 to initiate a coiled-coil when added to the N terminus of construct 6T. However, sedimentation equilibrium experiments showed that neither construct 2h6T nor construct 8T of identical length formed a coiled-coil.

If residues 1381–1393 are not a trigger sequence, another explanation must exist for the assembly differences between constructs 12T and 14T. These residues may stabilize the coiled-coils indirectly by allowing them to dimerize in the second step of myosin-II assembly. Perhaps 14T forms stable coiled-coils only when it dimerizes.

## Requirements for dimer formation

The minimal construct to form a dimer of coiled-coils is 14T, consisting of the C-terminal 14 heptads and tailpiece. Under all conditions, construct 12T, which is only 13 residues shorter than 14T, exists predominantly as single chains in weak equilibrium with coiled-coil monomers. Nevertheless, 12T is sufficiently well folded to crystallize at high concentration in the presence of PEG 8000.[20] However upon addition of one more heptad to 14T to form 15T, dimers are ten times more stable. Sedimentation equilibrium experiments showed

that constructs 15T, 15TC, and 15R all assemble into dimers with similar affinity in low salt. Since long constructs lacking the tailpiece form parallel dimers instead of antiparallel dimers,[3,11,17] we predict that the coiled-coils in 15R dimers are actually parallel. Sedimentation equilibrium does not reveal the geometry of these dimers, but a dramatic difference in the crystal form obtained for 15T and 15TC *versus* 15R suggests a different packing arrangement between these constructs.[20] Since both the tailpiece and residues between 1381 and 1393 are required for antiparallel dimerization, we hypothesize that the tailpiece binds its partner rod within this sequence, as expected from ~15 nm overlap observed in electron micrographs of rotary-shadowed samples.[1]

Residues 1381–1393 (heptads 13 and 14) and the tailpiece are necessary but not sufficient to form antiparallel dimers. Construct 2h6T includes both of these regions but does not form dimers. The addition of residues 1381–1393 to the N terminus of 6T continued the heptad repeat in-register but did not maintain the 28 residue charge pattern characteristic of all myosin-II tails (Figure 2). Since assembly is salt-dependent, we anticipate that the ionic interactions are crucial for dimerization. The lack of charge complementarity may compromise antiparallel dimerization of transiently formed coiled-coils.

Three tryptophan substitutions in 15T provide clues about the lateral interactions in dimers. A1378 must not be involved directly in the dimerization, since substitution of tryptophan at this position does not compromise dimerization or give a fluorescence change when the construct dimerized. Since A1378 is only five residues from the N terminus of 15T, it is possible that it is located outside the region of antiparallel overlap. Otherwise, it may be within the interaction region but oriented away from the dimerization interface. L1475 is likely to be buried in the interface between subunits in dimers, since substitution of tryptophan strongly inhibits dimerization. Only monomers were present under both the low-salt and high-salt conditions used to monitor fluorescence, so no signal was detected. F1443 is probably near the dimer interface, since the fluorescence of tryptophan at this position is altered by assembly, and since this substitution has a mild effect on assembly. In addition, F1443W does not crystallize under any conditions similar to 15T, indicating that the tryptophan also influences crystal packing contacts. Therefore, we expect that F1443 is located near the dimer interface but also accessible to the solvent. On the other hand, L1475W crystallizes similarly to 15T in spite of the low affinity for dimerization. Therefore, dimers can form under high concentrations of protein and precipitant, and the crystal packing is not affected by the tryptophan addition.

These biochemical data provide parameters to guide our structural understanding. Specifically, we have evidence that: (1) the tailpiece interacts with residues 1381–1393; (2) A1378 is outside of the interaction face; (3) L1475W inhibits dimerization; and (4) F1443 is involved in the dimerization interface but exposed to the solvent.

### Requirements to form tetramers and octamers

Previous work showed that myosin-II assembles by three steps of antiparallel dimerization producing overlapping regions of 15 nm in dimers, 30 nm in tetramers and 60 nm in octamers (Figure 1). Accordingly, we find that a 15 nm construct (14T) is required to form dimers and a 34 nm construct (32T) is sufficient to form tetramers. Constructs 20T and 22T form dimers, but not tetramers. Therefore, myosin-II tail constructs must include residues between 1254 and 1325 (heptads 23–32) to form tetramers. Since a monoclonal antibody bound to an epitope centered on residue 1278 allowed myosin-II to form tetramers but not octamers,[10] we propose that tetramerization involves residues between 1254 and 1278. Hypothetically a 30 nm construct beginning at residues 1278 (29T) would bridge the entire 30 nm interaction zone observed in tetramers. The ~15 nm stagger between myosin-II heads in minifilaments indicates that the tetramerization domain interacts with the antiparallel dimer formed in step 1 of assembly. Since assembly occurs only through successive steps of dimerization, we propose that the tetramerization site of each myosin-II tail binds a site created in the 15 nm antiparallel overlap between the two coiled-coils of the 15T dimer, an interaction among three coiled-coils. The 3D arrangement of this binding site remains to be established.

In addition to forming tetramers, 32T forms high-affinity octamers. In spite of its small size, construct 32T with just the C-terminal 256 residues (34 nm) faithfully mimics the assembly properties of the native protein. In live cells, a green fluorescent protein fusion to the N terminus of 32T incorporates into particles of two sizes that are interpreted to be minifilaments and thick filaments.[5] In low salt, the predominant 32T species is an octamer, which dissociates into dimers and tetramers in high salt. Like minifilaments of native myosin-II, 32T octamers aggregate in $MgCl_2$. Neither 20T nor 22T formed octamers. The inability of 22T and 20T to form tetramers precludes their formation of octamers and explains why they do not precipitate in $MgCl_2$. Construct 32T contains the N-terminal residues required to form minifilaments, including sequence around residue 1278, which is involved in octamer formation.[10]

Construct 32T is only 34 nm long compared to the observed maximum antiparallel overlap of 60 nm observed in rotary shadowed minifilaments. Since 32T forms octamers, the 34 nm coiled-coil construct is sufficient to span a 60 nm region. Therefore, it is not necessary for all eight molecules to physically interact in the final dimerization of tetramers to form octamers. Although Figure 1 is a simple 2D diagram, it makes the point that the top molecule on

the left is unlikely to interact with the bottom molecule on the right in octamers of 32T.

The longitudinal overlaps of molecules in rotary-shadowed minifilaments observed by electron microscopy suggested that the entire length of the tail might participate in forming octamers. Although the maximum antiparallel overlap is only 60 nm, the tails of molecules bordering the bare zone might interact with parallel tails along their entire length of 95 nm (663 residues) (Figure 1). The potential for the N-terminal 58 heptads to interact with neighboring tails is not detected. This suggests that the proline 1244 hinge may allow the proximal part of the tail to swing away from the backbone of the filament.

## Materials and Methods

### Cloning

Truncation constructs were obtained by PCR with the Elongase Enzyme Mix (Life Technologies, Inc.) using *Acanthamoeba* myosin-II cDNA as a template with primers generating various N and C termini (Figure 2). We designed a total of 13 N-terminal primers to produce constructs ranging in length from six to 32 heptads (Figures 2 and 3). Three C-terminal primers were designed to produce variable ends based on protein domains and proteolytic sensitive sites. The three C-terminal primers created constructs that included the entire tailpiece (T), lacked the last seven residues at a natural chymotryptic site (TC),[9] or lacked the entire non-helical tailpiece (R). Pairs of these 16 primers could be used in any combination to produce over 50 different constructs. Each construct was named, with a number indicating the number of heptad repeats and a letter designating the C-terminal end (for example, the construct consisting of 15 heptads and the full tailpiece is called 15T). PCR products were digested overnight at 37 °C with restriction enzymes NdeI and BamHI for cloning into the pMW172 expression vector.[21] To create point mutations, the entire vector was amplified using forward primers that contained 20–40 base-pairs of endogenous sequence plus a reverse primer that began just 5′ of the splice site. The resulting PCR product was phosphorylated and ligated into pMW172. Automated di-deoxy sequencing (ABI) was used to confirm the sequence for all plasmids with a PCR insert of the correct size that expressed protein of the correct molecular mass.

### Protein expression

We expressed constructs in *E. coli* BL21 (DE3) (Stratagene). We inoculated 1 l of TB medium (200 μg/ml of carbenicillin) in a fluted culture flask with a single colony from a fresh transformation (less than 48 hours old) and grew the culture overnight at 37 °C with shaking at 220 rpm. In spite of the T7 promoter in pMW172, the bacteria expressed a large quantity of protein without induction by IPTG. Cells were collected after 12–18 hours (20–30 hours for construct 6T) by centrifugation at 6000*g* for 20 minutes and frozen at −80 °C. We added 50 ml of lysis buffer (10 mM Tris, 10 mM EDTA, 10% (w/v) sucrose, 0.01% (v/v) Triton X-100, 1 mg/ml of lysozyme, 1 mM PMSF) to the frozen cell pellet, stirred the pellet until it thawed, and then sonicated the pellet until it was no longer viscous (0.5 s alternating pulse for 30 s, repeated eight times). The lysate was transferred to a 250 ml Erlenmeyer flask with a stir bar and suspended in a boiling waterbath for ten minutes with stirring. After chilling on ice for one hour, the supernatant containing the expressed protein was isolated by centrifugation at 75,000*g* for one hour. While most globular proteins were denatured and removed in the pellet, the coiled-coil proteins remained in the supernatant, as shown previously for tropomyosin[22] and bacterially expressed myosin tail constructs.[23–25]

### Protein purification

We dialyzed boiled supernatant against 20 mM Tris (pH 8), 1 mM EDTA and loaded it onto a 50 ml DEAE column equilibrated in the same buffer. Protein was eluted with 150 ml of 20 mM Tris (pH 8), 1 mM EDTA, 100 mM KCl. Under these conditions, nucleic acids bound to the column. The enriched protein pool from the DEAE column was dialyzed into 20 mM imidazole (pH 7), 1 mM EDTA. Cation-exchange chromatography was then performed in the same buffer on a Mono S FPLC column (Pharmacia). A gradient of 0–150 mM KCl eluted myosin-II constructs near 80 mM KCl. We concentrated the protein using Centriprep-3 membrane concentrating devices (Amicon Inc.) in 10 mM Tris (pH 7.5), 1 mM EDTA. For constructs 32T, 22T, and 20T, 100 mM KCl was required to keep the protein in solution at high concentrations. The purity of the protein was checked by staining of SDS-15% PAGE gels with Coomassie brilliant blue.

To purify construct 32T, the supernatant from cell lysis was dialyzed overnight into 20 mM Tris (pH 7.5), 5 mM $MgCl_2$. The fine white precipitate that appeared was collected by centrifugation at 6000*g* for 15 minutes. We gently resuspended the pellet in 10 ml of 10 mM Hepes (pH 8), 40 mM sodium pyrophosphate, 10 mM EDTA. After centrifugation at 6000*g* for 15 minutes, the supernatant was loaded onto the DEAE column to remove nucleic acids.

For isoelectric focusing of construct 15T, fractions from the Mono S column were denatured in 4 M urea and then loaded onto an 0.5% (w/v) agarose gel with 2% (v/v) pH 3–9 ampholines (Pharmacia) and 10% (w/v) sorbitol cast onto Gelbond (Pharmacia) support matrix. The samples were focused on a flatbed unit with cathode buffer of 0.5 M NaOH and anode buffer of 0.5 M glacial acetic acid until the current reached a minimum. The gel was fixed in 10% (v/v) trichloroacetic acid and 5% (v/v) sulfosalicylic acid, rinsed in ethanol to remove the ampholines, partially dried with a hair-dryer, and stained with Coomassie brilliant blue.

Since most constructs lacked residues that absorbed at 280 nm, we identified protein in column fractions using the Bio-Rad Protein Assay (Bio-Rad Laboratories). The tryptophan point mutant 15T-F1443W had an estimated extinction coefficient of 5690 $M^{-1}\,cm^{-1}$ at 280 nm and was used for standard curves. Since construct 6T did not react with the Bio-Rad reagent but stained well with Coomassie brilliant blue on SDS/polyacrylamide gels, we used a filter-paper dye-binding assay for quantification.[26]

### Analytical ultracentrifugation

Molecular mass was determined by sedimentation equilibrium analytical ultracentrifugation. Samples were placed in six-hole, charcoal-filled Epon centerpieces and maintained at 20 °C. Centrifugation to equilibrium

required up to 36 hours at each speed in an An60 Ti rotor with a Beckman Optima XLI ultracentrifuge (Beckman Instruments). Rotor speeds were selected to optimize the sedimentation curve for fitting based on the size of the expected species with a twofold increase in the speed factor between rotor speeds. We monitored the approach to equilibrium using interference optics to collect data every hour and calculated the root-mean-square (RMS) deviation between sets using Matchv7 software (Jeff Lary, National Analytical Ultracentrifuge Facility, Storrs, CT). The program Reedit9 (Jeff Lary, National Analytical Ultracentrifuge Facility, Storrs, CT) truncated and saved each curve separately, based on its starting concentration and rotor speed. All the data sets for a particular construct under the same buffer conditions were fit globally to obtain the effective reduced molecular mass and equilibrium constants using the program WinNonlin.[27] The value of $M_z$ was obtained by fitting the data globally to a single species, rather than an equilibrium between multiple species. This value provided a starting point for fitting to association reactions. We tried fits between all combinations of monomer, dimer, trimer, and tetramer and compared residuals to determine the best fit.

### Light-scattering

Assembly was monitored by 90° light-scattering in a fluorescence spectrophotometer (PTI Alphascan, Photon Technology International Inc., So. Brunswick, NJ). A concentrated protein stock solution was dialyzed into 20 mM Tris (pH 8) and passed through a 0.22 μm pore size filter. Excitation and emission wavelengths were 365 nm with a wavelength range of 0.75 nm. The concentration of salt was varied up to 500 mM KCl by adding filtered 20 mM Tris (pH 8), 500 mM KCl. After measuring the light-scattering of the sample in a 1 cm×1 cm quartz cuvette, each value was normalized by subtracting the light-scattering of buffer alone.

### Fluorimetry

We measured fluorescence emission spectra of tryptophan mutants upon excitation at 290 nm using a PTI Alphascan. Since the absolute signal varied with time and with mixing, we used the ratio of the emission at 320 nm and 365 nm to compare samples over a range of concentrations of KCl between 0 and 2 M. Protein and buffer solutions were passed through a 0.45 μm pore size filter.

### Circular dichroism spectroscopy

Purified construct 6T was dialyzed into 5–200 mM pyrophosphate and placed in a 0.5 mm cell. CD spectra were recorded at 22 °C from 260 nm and 190 nm using an AVIV model 62DS spectropolarimeter (AVIV Associates, NJ) and the manufacturer's 60DS software. No post-collection smoothing was applied to the data. Buffer spectra were subtracted from sample spectra. Using the concentration of 6T determined by the filter-paper dye-binding assay, the raw data were converted to mean residue ellipticity. Spectral deconvolutions employed the program PROSEC.[28]

## Acknowledgements

We thank Mark Yeager for helpful discussions and a critical reading of the manuscript. This work was supported by NIH research grant GM26132.

## References

1. Pollard, T. D. (1982). Structure and polymerization of *Acanthamoeba* myosin-II filaments. *J. Cell Biol.* **95**, 816–825.
2. Sinard, J. H., Stafford, W. F. & Pollard, T. D. (1989). The mechanism of assembly of *Acanthamoeba* myosin-II minifilaments: minifilaments assemble by three successive dimerization steps. *J. Cell Biol.* **109**, 1537–1547.
3. Sinard, J. H. & Pollard, T. D. (1990). *Acanthamoeba* myosin-II minifilaments assemble on a millisecond time scale with rate constants greater than those expected for a diffusion limited reaction. *J. Biol. Chem.* **265**, 3654–3660.
4. Yonemura, S. & Pollard, T. D. (1992). The localization of myosin I and myosin II in *Acanthamoeba* by fluorescence microscopy. *J. Cell Sci.* **102**, 629–642.
5. Kong, H.-H. & Pollard, T. D. (2002). Intracellular localization and dynamics of myosin-II and myosin-IC in live Acanthamoeba by transient transfection of EGFP fusion proteins. *J. Cell Sci.* **115**, 4993–5002.
6. Hammer, J. A., III, Bowers, B., Paterson, B. M. & Korn, E. D. (1987). Complete nucleotide sequence and deduced polypeptide sequence of a nonmuscle myosin heavy chain gene from *Acanthamoeba*: evidence of a hinge in the rodlike tail. *J. Cell Biol.* **105**, 913–925.
7. Parry, D. A. (1981). Structure of rabbit skeletal myosin. Analysis of the amino acid sequences of two fragments from the rod region. *J. Mol. Biol.* **153**, 459–464.
8. McLachlan, A. D. & Karn, J. (1983). Periodic features in the amino acid sequence of nematode myosin rod. *J. Mol. Biol.* **164**, 605–626.
9. Côté, G. P., Robinson, E. A., Appella, E. & Korn, E. D. (1984). Amino acid sequence of a segment of the *Acanthamoeba* myosin II heavy chain containing all three regulatory phosphorylation sites. *J. Biol. Chem.* **259**, 12781–12787.
10. Rimm, D. L., Kaiser, D. A., Bhandari, D., Maupin, P., Kiehart, D. P. & Pollard, T. D. (1990). Identification of functional regions on the tail of *Acanthamoeba* myosin-II using recombinant fusion proteins. I. High resolution epitope mapping and characterization of monoclonal antibody binding sites. *J. Cell Biol.* **111**, 2405–2416.
11. Sinard, J. H., Rimm, D. L. & Pollard, T. D. (1990). Identification of functional regions on the tail of *Acanthamoeba* myosin-II using recombinant fusion proteins. II. Assembly properties of tails with $NH_2$- and COOH-terminal deletions. *J. Cell Biol.* **111**, 2417–2426.
12. Sinard, J. H. & Pollard, T. D. (1989). The effect of heavy chain phosphorylation and solution conditions on the assembly of *Acanthamoeba* myosin-II. *J. Cell Biol.* **109**, 1529–1535.
13. Lupas, A., Van Dyke, M. & Stock, J. (1991). Predicting coiled coils from protein sequences. *Science*, **252**, 1162–1164.
14. Lupas, A. (1997). Predicting coiled-coil regions in proteins. *Curr. Opin. Struct. Biol.* **7**, 388–393.
15. Su, J. Y., Hodges, R. S. & Kay, C. M. (1994). Effect of chain length on the formation and stability of synthetic α-helical coiled coils. *Biochemistry*, **33**, 15501–15510.
16. O'Shea, E. K., Klemm, J. D., Kim, P. S. & Alber, T.

(1991). X-ray structure of the GCN4 leucine zipper, a two-stranded, parallel coiled coil. *Science*, **254**, 539–544.
17. Kuznicki, J., Cote, G. P., Bowers, B. & Korn, E. D. (1985). Filament formation and actin-activated ATPase activity are abolished by proteolytic removal of a small peptide from the tip of the tail of the heavy chain of *Acanthamoeba* myosin II. *J. Biol. Chem.* **260**, 1967–1972.
18. Chang, C. T., Wu, C.-S.C. & Yang, J. T. (1978). Circular dichroic analysis of protein conformation: inclusion of the β-turns. *Anal. Biochem.* **91**, 13–31.
19. Kammerer, R. A., Schulthess, T., Landwehr, R., Lustig, A., Engel, J., Aebi, U. & Steinmetz, M. O. (1998). An autonomous folding unit mediates the assembly of two-stranded coiled coils. *Proc. Natl Acad. Sci. USA*, **95**, 13419–13424.
20. Turbedsky, K., Pollard, T. D. & Yeager, M. (2005). Assembly of *Acanthamoeba* myosin-II minifilaments. model of anti-parallel dimers based on EM and X-ray diffraction of 2D and 3D Crystals. *J. Mol. Biol.* (this issue).
21. Way, M., Pope, B., Gooch, J., Hawkins, M. & Weeds, A. G. (1990). Identification of a region in segment 1 of gelsolin critical for actin binding. *EMBO J.* **9**, 4103–4109.
22. Hitchcock-DeGregori, S. E. & Heald, R. W. (1987). Altered actin and troponin binding of amino-terminal variants of chicken striated muscle α-tropomyosin expressed in *Escherichia coli*. *J. Biol. Chem.* **262**, 9730–9735.
23. Atkinson, S. J. & Stewart, M. (1991). Expression in *Escherichia coli* of fragments of the coiled-coil rod domain of rabbit myosin: influence of different regions of the molecule on aggregation and para-crystal formation. *J. Cell Sci.* **99**, 823–836.
24. McNally, E., Sohn, R., Frankel, S. & Leinwand, L. (1991). Expression of myosin and actin in *Escherichia coli*. *Methods Enzymol.* **196**, 368–389.
25. O'Halloran, T. J., Ravid, S. & Spudich, J. A. (1990). Expression of *Dictyostelium* myosin tail segments in *Escherichia coli*: domains required for assembly and phosphorylation. *J. Cell Biol.* **110**, 63–70.
26. Minamide, L. S. & Bamburg, J. R. (1990). A filter paper dye-binding assay for quantitative determination of protein without interference from reducing agents or detergents. *Anal. Biochem.* **190**, 66–70.
27. Johnson, M. L., Correia, J. J., Yphantis, D. A. & Halvorson, H. R. (1981). Analysis of data from the analytical ultracentrifuge by nonlinear least-squares techniques. *Biophys. J.* **36**, 575–588.
28. Yang, J. T., Wu, C. S. & Martinez, H. M. (1986). Calculation of protein conformation from circular dichroism. *Methods Enzymol.* **130**, 208–269.

***Edited by W. Baumeister***

*(Received 25 August 2004; accepted 18 October 2004)*